Ophiolites from the Grammos-Arrenes area, northern Greece:geological, paleontological and geochemical data

OPHIOLITES FROM THE GRAMMOS-ARRENES AREA, NORTHERN GREECE: GEOLOGICAL, PALEONTOLOGICAL AND GEOCHEMICAL DATA

Giuseppe Nirta*,✉, Valerio Bortolotti*, Marco Chiari°, Francesco Menna*, Emilio Saccani, Gianfranco Principi*,° and Paola Vannucchi***

* *Dipartimento di Scienze della Terra, Università di Firenze, Italy.*
** *Dipartimento di Scienze della Terra, Università di Ferrara, Italy.*
° *C.N.R., Istituto di Geoscienze e Georisorse, U.O di Firenze, Italy.*
✉ *Corresponding author, e-mail: giuseppe.nirta@unifi.it*

Keywords: *basalt, radiolarian chert, ophiolite, flysch, mélange, Jurassic. Greece.*

ABSTRACT

The Grammos-Arrenes ophiolites crop out between the Pindos Flysch to the East and the Meso-Hellenic basin to the West and represent the northernmost exposure of the Pindos Ophiolite belt in Greece. Field work and sampling on key outcrops of the Sub-ophiolitic Mélange provided new data on the oceanization age and on the geochemistry of the effusive products. The basalts samples show a N-MOR affinity and are associated with latest Bajocian-early Bathonian radiolarian cherts.

Emplacement of the ophiolites onto the continental margin is preceded by mass flow deposition of ophiolitic material in the basins facing the advancing ophiolitic nappe. Ophiolite-bearing debris flow deposits and slide blocks are recognized in the Lower Cretaceous deep water sediments of the Beotian Unit and in the upper portion of the Tertiary Pindos Flysch. The intercalations of ophiolitic material in the Beotian Flysch first, and in the Pindos Flysch, later, are interpreted as the forerunners of the Ophiolitic Nappe which derived from the Vardar Ocean to the east, and was emplaced westwards onto the Adria continental margin.

The collected data allow consolidating the constraints for the timing and mechanism of ophiolite emplacement in the Pindos-Grammos area. In addition, taking into consideration the geometry of the tectonic stack in the Grammos-Arrenes area and the ages of the involved sedimentary deposits it is possible to reconstruct a geodynamic history comparable to that of the other zones studied along the Dinaric-Hellenic Chain.

INTRODUCTION

Ophiolites of the Dinaric-Hellenic belt are continuously exposed along 1000 km from Bosnia-Herzegovina to southern Greece, thus representing one of the largest ophiolite outcrops in the world (Fig. 1). Although many studies have been carried out on these ophiolites, a number of unresolved issues remain in the reconstruction of their evolution. A first discussion topic concerns the paleogeographic position of these ophiolites. Two main reconstructions have been proposed by different authors: **a**- a para-autochthonous origin reflecting their present tectonic configuration; **b**- a tele-allochthonous origin envisaging the existence of a far-travelled ophiolitic nappe. In the first reconstruction the Pindos-Grammos-Arrenes ophiolites were located between the Adria margin to the SE and a Pelagonian microcontinent to the NE, separating the Pindos oceanic basin from the wider Vardar Ocean (Smith et al., 1975; Jones and Robertson, 1991; Robertson, 2002). In the second reconstruction all the Greek ophiolites represent the remnants of a single ophiolitic nappe coming from the Vardar Ocean to the east, that overthrust the eastern margin of Adria (Bernoulli and Laubscher, 1972; Bortolotti et al., 2004b, Bortolotti and Principi, 2005). In the second hypothesis, the Pelagonian Zone represents the easternmost sector of the Adria passive margin.

The ophiolites cropping out between the Grammos Massif to the North, and the Arrenes area to the South represent the northernmost outcrops in Greece of the so called external ophiolite belt (Pindos Zone *sensu* Brunn, 1956 and Aubouin, 1959, Fig. 1), regarded as a link between the Albanian and Greek ophiolites. We here present new geochemical and biostratigraphic data from basalt and radiolarian chert samples and frame them in the Mesozoic evolution of the Dinaric-Hellenic Chain.

GEOLOGICAL SETTING

The closure of the Jurassic Tethys Ocean is recorded by the Dinaric-Hellenic ophiolite belt, a major segment of the Alpine-Himalayan mountain chain in the Eastern Mediterranean. Ophiolite rocks from the Grammos-Arrenes area in northwestern Greece record a Mesozoic history of subduction, accretion and obduction. The complex history of this area is registered in four main tectonic units derived from both oceanic and continental domains, they are, from top to bottom (Figs. 2, 3): Ophiolitic Nappe, Sub-ophiolitic Mélange, Beotian Unit and Pindos Flysch Unit. Above the Ophiolitic Nappe and the Sub-ophiolitic Mélange a thick carbonate sequence (Late Cretaceous in age) is present. Moreover, in this area the thrust sheets have been unconformably covered by the Tertiary molasses of the Meso-Hellenic intermontane basin. The Pindos-Grammos ophiolites represent the continuation below the Meso-Hellenic basin, of the Vourinos ophiolites to the East (Moores, 1969).

All the ophiolites along the Dinaric-Hellenic Chain show evidences to have been emplaced onto a passive margin through an obduction process (Gaggero et al., 2009), as also recognized for many Tethyan ophiolites of the Eastern Mediterranean and Middle East (e.g., Semail ophiolites in Oman, Searle and Cox, 1999). Greenschist to amphibolite facies metamorphic rocks formed at the base of the Pindos Ophiolitic Nappe as the effect of intraoceanic displacement of a young and hot oceanic crust during the Middle Jurassic (165±3 Ma, Spray et al., 1984).

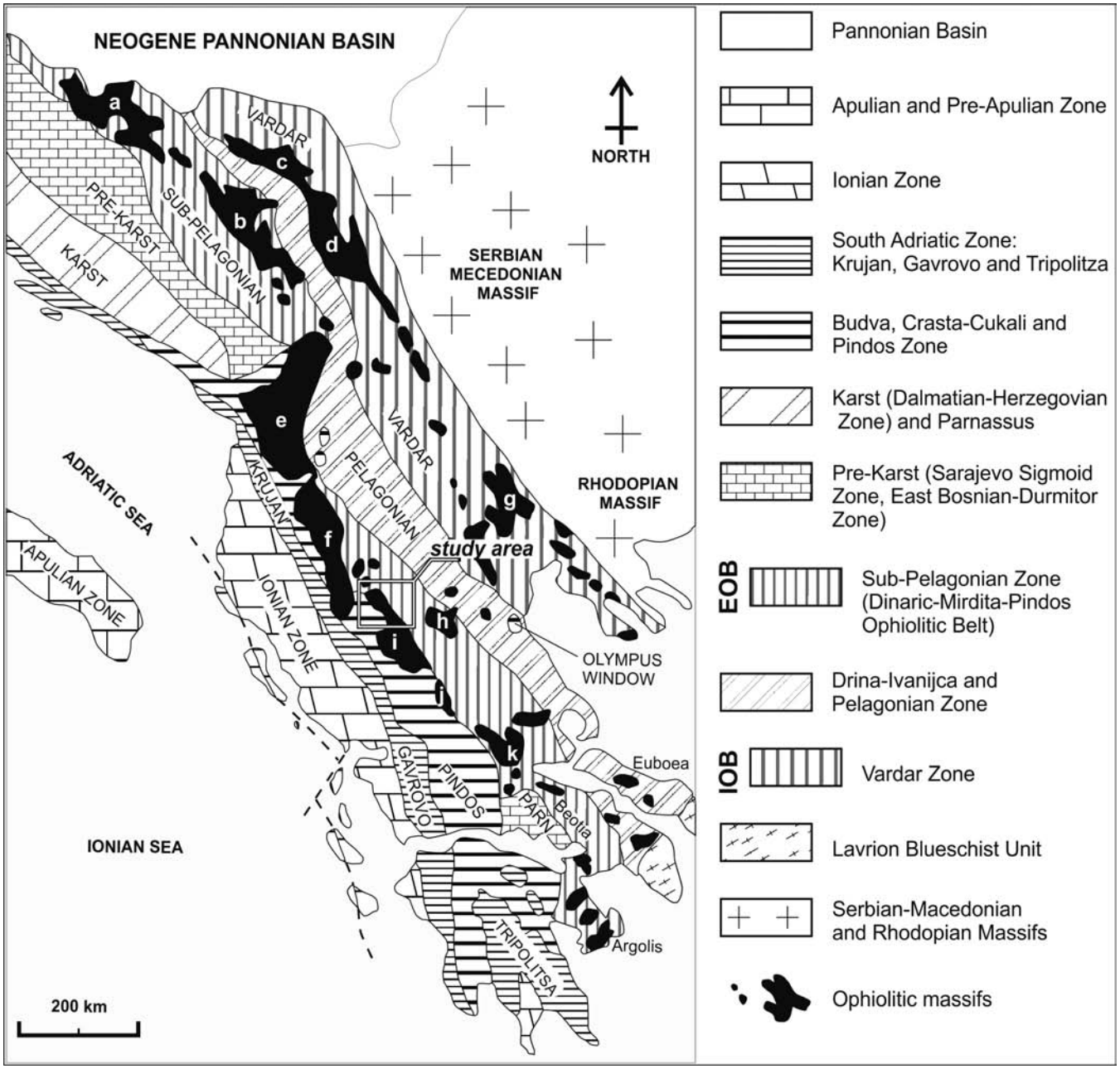

Fig. 1 - Tectonic sketch map of the Dinaric-Hellenic Belt with the main tectono-stratigraphic units. PARN-Parnassus Zone. EOB- External Ophiolitic Belt; IOB- Internal Ophiolitic Belt. Main ophiolitic massifs: a- Krivaja-Konjuh; b- Zlatibor; c- Maljen; d- Ibar; e- Mirdita; f- Shpati-Devolli-Korca; g- Guevgeli; h- Vourinos; i- Pindos-Arrenes-Grammos; j- Koziakas; k-Othris. The study zone is indicated in the boxed area. Modified after Bortolotti et al. (2004b).

In the Grammos-Arrenes area, the Ophiolitic Nappe includes harzburgitic mantle tectonites, ultramafic cumulates, gabbros and basalts. The basalts are covered by a cm- to dm-thick level of siliceous shale followed by radiolarian cherts. The exposure of a metamorphic sole under the ophiolites is discontinuous and consists of a < 1 m thick continuous band of mesoscopically not foliated metamorphic rocks overlying a discontinuous, usually thick assemblage of metasediments and amphibolites. Below the Ophiolitic Nappe, the Sub-ophiolitic Mélange is characterized by an upper portion of tectonic origin with a very low grade metamorphic assemblage of ophiolites and a lower portion largely built by gravitational mechanisms with elements of the metamorphic sole, ophiolites and continental-derived blocks embedded in the debris flow deposits.

The Sub-ophiolitic Mélange and the Ophiolitic Nappe are overthrust by a thick sequence of platform carbonates of Santonian-Campanian age (Orliakas Group, Brunn, 1956; Jones and Robertson, 1991). Locally, the basal contact of the carbonate sequence on the ophiolitic basement is highlighted by a metric reddish horizon of laterites that unconformably cover the ophiolites. The Ophiolitic Nappe + Sub-ophiolitic Mélange overthrust discontinuous slices of Early Cretaceous continental margin sequences, mostly consisting of deep water carbonate, shale, radiolarite and ophiolite-bearing debris flow deposits (Agios Nikolaos Formation, Jones and Robertson, 1991). The stratigraphy of this sequence and its age (Berriasian-?Hauterivian, Terry and Mercier, 1971; Richter and Müller, 1992) allow a correlation with the upper sequence of the Beotian Zone that is

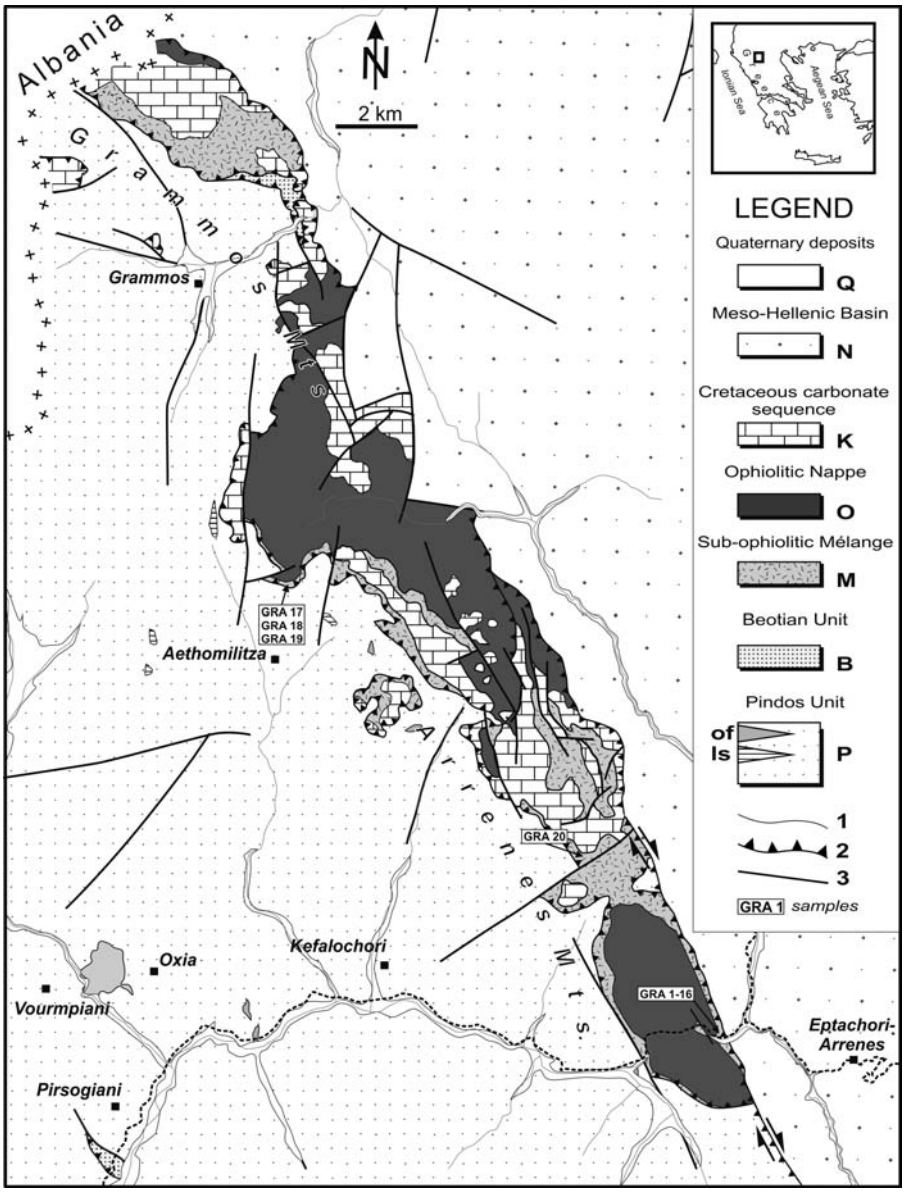

Fig. 2 - Geological and structural sketch map of the Grammos-Arrenes area. Q- Quaternary alluvial deposits. N- Neogene deposits of the Meso-Hellenic Basin. K- Upper Cretaceous carbonate sequence. O- Ophiolitic Nappe (mainly serpentinites). M- blocks of ophiolites, amphibolites and continental-derived material enveloped in a shaly matrix mainly consisting of sheared mass flow deposits. B- Lower Cretaceous deep water carbonate and shale with ophiolite-bearing debris flow deposits. P- Paleocene-Eocene Flysch, of- ophiolite slide blocks and debris flow deposits, ls- Cretaceous limestone slide blocks. 1- stratigraphic contact; 2- thrust; 3- fault. Modified after IGME (1985), IGME (1987) and Richter and Müller, 1992.

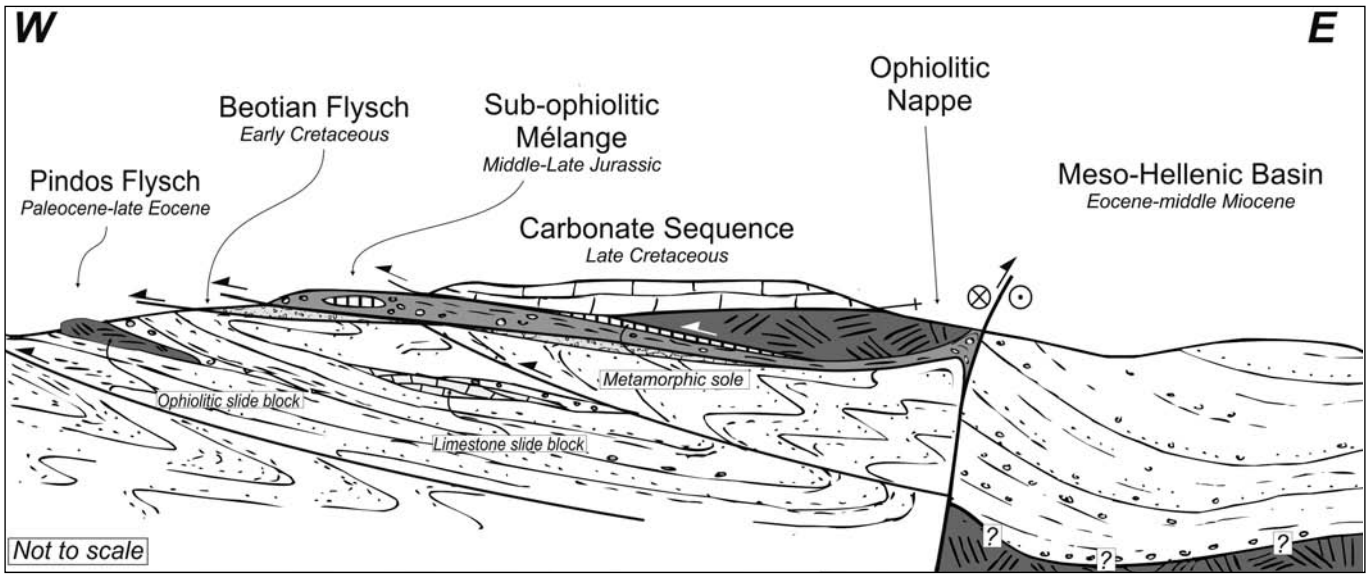

Fig. 3 - Schematic geologic cross section across the Grammos-Arrenes area.

interpreted as the westward extension of the Pelagonian platform (Robertson et al., 1991; Richter and Müller, 1992; Thiébault et al., 1994; Danelian and Robertson, 1998). The ophiolite-bearing deposits at the top of the Beotian sequence, known as Beotian Flysch were shed in front of the advancing Ophiolitic Nappe, thus dating the obduction onto the Pelagonian continental margin to the Late Jurassic (Richter et al., 1996). Ophiolite-bearing turbidite deposits of Early Cretaceous age with the same paleogeographic significance of the Beotian Flysch are recognized all along the Dinaric-Hellenic Chain (Bosnian Flysch, Blanchet et al., 1969; Firza Flysch, Gardin et al., 1996; Vermosh Flysch, Marroni et al., 2009). From a regional point of view the ophiolite-bearing detritus in the Pelagonian sequences show a younging direction from the Maliac-Othrys area to the Beotia area suggesting a westward emplacement direction of the Ophiolitic Nappe (De Bono, 1998 and reference therein).

The Paleocene - Late Eocene Pindos Flysch (Ananiadis et al., 2004), is regarded as a foreland basin deposit, which was progressively overthrust westwards-by the Sub-ophiolitic Mélange + Ophiolitic Nappe (Fig. 4a). This event is recorded in the turbiditic sediments by diffuse syn-sedimentary deformations and catastrophic events of mass deposition – mega-debris flows and slide blocks – with provenance from both continental margin units (Fig. 4a) and ophiolitic units (Fig. 4b; Bortolotti et al., 2009). In the Grammos-Arrenes area, the flysch crops out as a folded unit, when strongly deformed showing a broken formation appearance.

DESCRIPTION OF THE SAMPLED AREAS

Samples of radiolarian cherts, basalts and greenschist to amphibolite metamorphic rocks were collected in the Sub-ophiolitic Mélange. A detailed sampling was performed along a 30 m-wide outcrop of mélange along the Ioannina-Kozani road (samples GRA1 to GRA16). Other samples were collected in scattered outcrops in the Grammos-Arrenes Mountains (samples GRA17 to GRA20) (Fig.2).

The outcrop along the Ioannina-Kozani road (Fig. 4c, Fig. 5) exposes the base of a serpentinite thrust sheet (the Ophiolitic Nappe) that lies on an assemblage of sheared debris flow deposits and magmatic (locally metamorphosed)

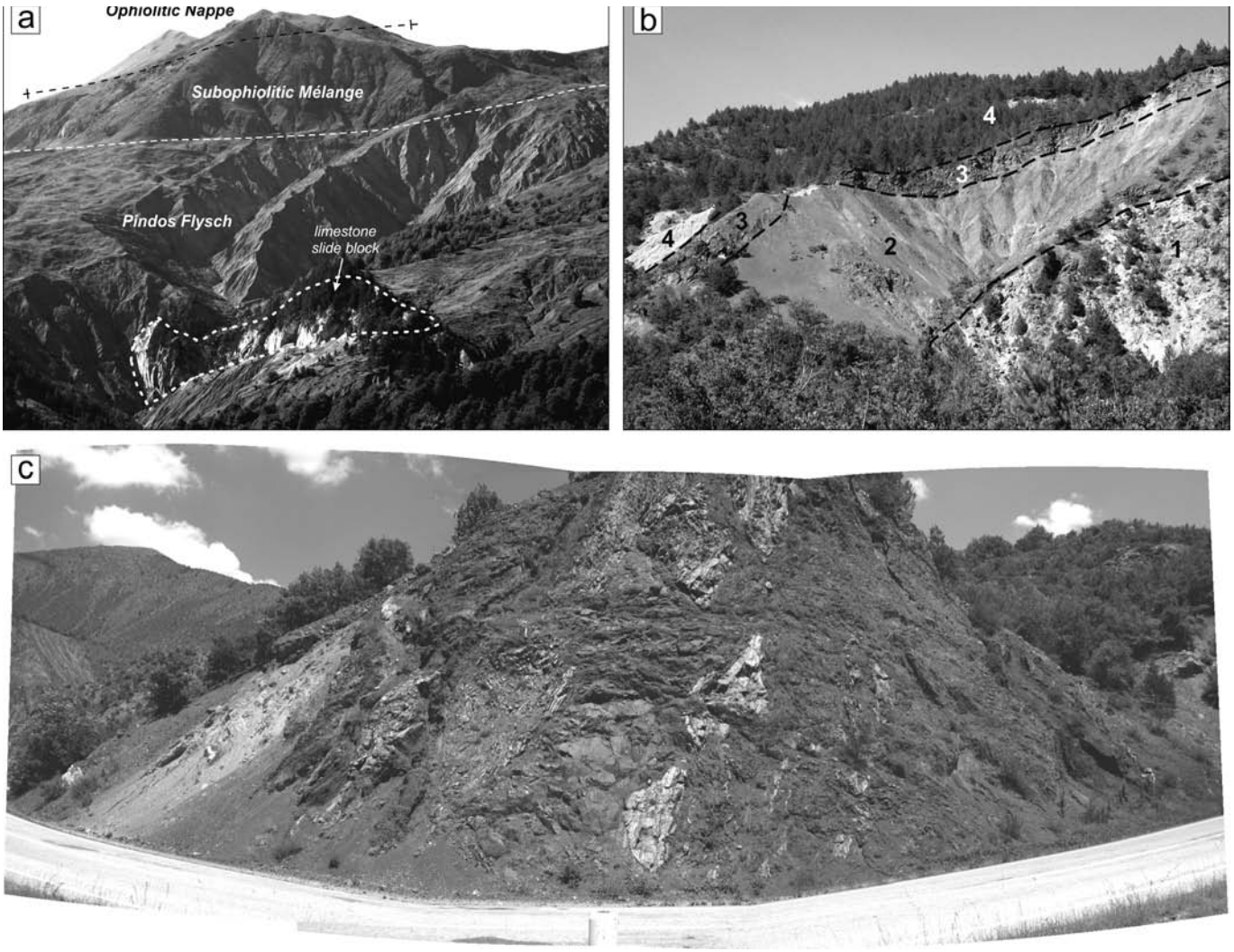

Fig. 4 - a- Tectonic superposition of the Ophiolitic Nappe, Sub-ophiolitic Mélange and Pindos Flysch in the Aetomilitsa area; b- mass flow deposits of ophiolitic material in the upper portion of the Pindos Flysch (Oxia area). 1- granular mega-debris flow deposit with ophiolitic elements ranging from cm up to tens of meters in size; 2- ophiolitic cohesive debris flow deposit; 3- ophiolitic granular debris flow deposit with elements ranging in size from cm to few meters; 4- Pindos Flysch with widespread syn-sedimentary deformations; c- sampled mélange outcrop along the Ioannina-Kozani road (see line drawing in Fig. 5 for explanation).

rocks, mainly including dolerite, basalt and serpentinite, associated with sedimentary rocks, such as limestone and radiolarite. The contacts among the different lithotypes (e.g., between carbonates and radiolarite or basalt, as well as those between serpentinite and debris flow deposits) are generally tectonic or tectonized because of the occurrence of several shear zones, especially developed along the lithologic boundaries. Nevertheless, a possible stratigraphic origin cannot be excluded for any of the mentioned contacts. A primary sedimentary contact is observed between basalts and radiolarites, while a primary magmatic contact can be assumed between the dolerite intrusion and the limestone. In fact, the dolerite mass partially includes the limestone, represented by some centimetres up to 2-3 meters thick disarticulated carbonatic bodies, internally characterized by regular, closely-spaced sedimentary bedding. Close to the lithologic boundary, 1-3 cm thick dark reaction borders developed in the carbonatic levels, mainly consisting of a garnet and pyroxene association.

The carbonatic rocks are recrystallized and transformed into marbles. The dolerite, essentially made of clinopyroxene and plagioclase, is characterized by an isotropic to foliated texture, with a medium-fine grain size. A foliation is well detectable in most outcrops of these lithologies. The serpentinite is characterized by a discontinuous foliation, variously penetrative at a mm/cm scale.

Other samples were collected in the Sub-ophiolitic Mélange along the contact with the underlying Pindos Flysch in the Aetomilitsa area and in the Arrenes Mountains (GRA17-20). The mélange in these areas consists of a shaly matrix, in some cases represented by sheared debris flow deposits, embedding slivers of limestones, cherts, basalts, serpentinites and greenschist/sub-greenschist (GRA 19-20) to granulite facies (GRA17-18) metamorphic rocks.

PETROGRAPHY AND GEOCHEMISTRY

Petrography

All the basaltic samples (GRA6-7, GRA15-16) were affected by high degrees of ocean-floor hydrothermal alteration under static, lower greenschist facies conditions, which has resulted in a complete re-crystallization of the primary igneous phases. Plagioclase has been replaced by either albite or clay minerals, clinopyroxene has been transformed into chlorite, and glass has been re-crystallized as clay minerals. By contrast, the primary igneous textures are well preserved. The studied basalts show very fine-grained aphyric texture with hyalophitic groundmass. Groundmass mineral assemblages include thin laths of plagioclase and interstitial clinopyroxene and glass. Such a texture testifies for the early crystallization of plagioclase with respect to clinopyroxene. These volcanic rocks are also characterized by sparse calcite veins.

The dolerite intrusion (GRA11; Fig. 5) is composed by plagioclase and clinopyroxene (diopside) inside which are present some intergrowths, now transformed into chlorite. Ilmenite, Ti-oxide, chrome and spinel are also present. Dolerite is generally characterized by a micro-granular ipidiomorphic texture, with idiomorphic plagioclase and interstitial to poikilitic clinopyroxene (Fig. 6a). The magmatic foliation is underlined by the albite and albite-Carlsbad twinning of the plagioclase. Low-temperature mineral assemblages, crystallized under static conditions, are widespread: amphiboles such as tremolite, are often pseudomorphic after magmatic clinopyroxene plagioclase is altered into a fine-grained assemblage of albite, epidote, prehnite and sericite.

The limestones (GRA5; Fig. 5) enclosed in the doleritic intrusion are transformed in marble with a granoblastic texture. The metamorphic mineral assemblages contain calcite, garnet, vesuvianite and clinopyroxene. At the contact with the magmatic body it can be recognized a centimetric (1-3 cm) reaction rim essentially made of granoblastic level of garnet and clinopyroxene.

Centimetric to decimetric gabbro-derived granulite slices in the Sub-ophiolitic Mélange (GRA17-18; Fig. 2) show high-temperature metamorphic recrystallization, evidenced by the development of a tectonic pervasive foliation, at the sub-millimetric/millimetric scale, marked by alternating plagioclase and pyroxenes levels. Plagioclase forms polygonal aggregates with 120° triple junctions. Clinopyroxenes are recrystallized into aggregates of secondary syn-kinematic neoblastic clinopyroxene, with 120° triple junctions associated with minor brown amphibole ± ilmenite ± brown spinel.

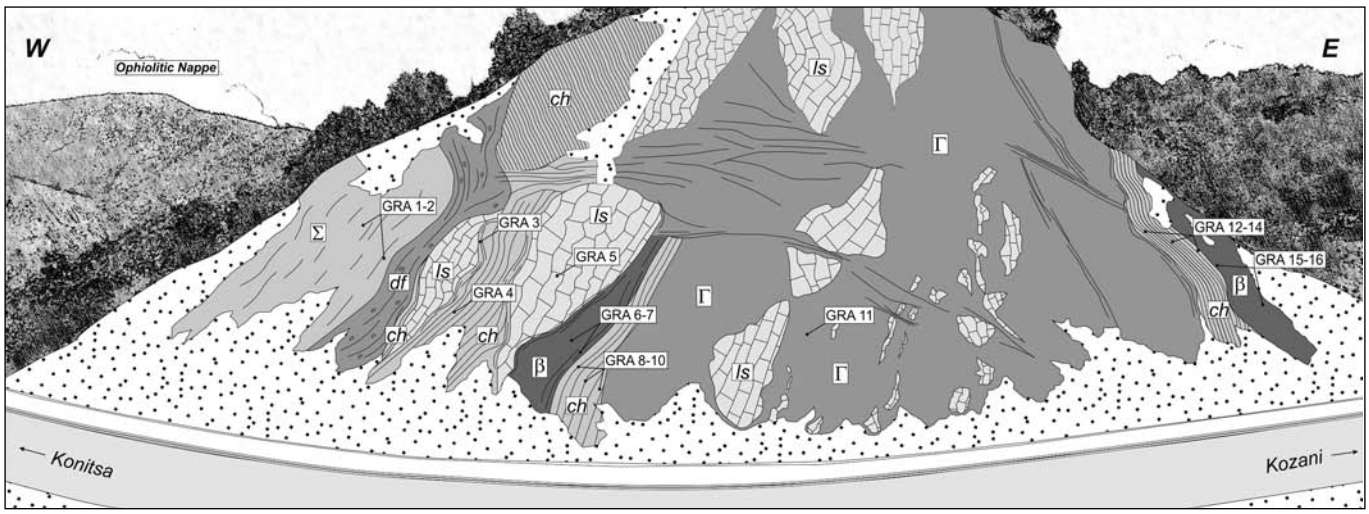

Fig. 5 - Mélange outcrop sampled along the Ioannina-Kozani road. The "volcano-sedimentary" sequence, though intensively sheared, is partly preserved. Σ- serpentinite; df- sheared debris flow deposit; β- basalt; ch- radiolarian chert and siliceous shale; ls- metamorphosed limestone; Γ- doleritic intrusion.

The petrographical and textural features of the serpentinites (GRA1-2; Fig. 5) indicate an origin from mantle peridotites. Serpentinization affected olivine and orthopyroxene, whereas clinopyroxene and spinel occur as mineral relics. The serpentinites display an "orogenic\post-orogenic" pervasive tectonic foliation related to ductile and brittle shear zones, developed in greenschist to sub-greenschist metamorphic conditions. The shear zones are characterized by a textural and mineralogic reorganization that causes the development of mylonitic fabrics associated with a foliation marked by lepidoblastic/nematoblastic tremolite and actinolite levels.

In the phyllites and calcschists sampled at the contact between Sub-ophiolitic Mélange and Pindos Flysch (GRA19-20; Fig. 2), two deformational phases (D_1 and D_2) were recognized. The D_1 phase produced the S_1 foliation corresponding to a slaty cleavage marked by the alternation of quartz-feldspar-calcite-rich and phyllosilicate-rich layers, consisting of fine-grained intergrowth of white mica and chlorite. No folding structures associated with this foliation were recognized. The S_1 foliation is made of greenschist facies mineral assemblages (muscovite + sericite + calcite + chlorite + quartz). The D_2 phase folding event (Fig. 6b) generated the S_2 foliation that consists in a crenulation cleavage, where the S_1 foliation is preserved as relict foliation in microlithons. The S_2 mm-spaced axial plane foliation is made of greenschist to sub-greeschist facies mineral assemblages (chlorite + quartz + opaque).

Analytical methods

Bulk-rock major and trace element analyses on the two basaltic samples (GRA15-16; Fig. 5) that are stratigraphically associated with radiolarites were performed by X-ray fluorescence (XRF) and by inductively coupled plasma-mass spectrometry (ICP-MS) at the Department of Earth Sciences of the University of Ferrara. Samples GRA6 and GRA7 were not analysed because it was not possible to assign and age to the associated radiolarian chert samples due to their bad preservation. Chemical compositions are presented in Table 1. The XRF analyses were performed on pressed powder pellets with an ARL Advant-XP automated spectrometer using the matrix correction methods proposed by Lachance and Trail (1966). The ICP-MS analyses were achieved using a VG Elemental Plasma Quad PQ2 Plus spectrometer. Accuracy for XRF analyses is better than 3% for Si, Ti, Ca, K and 7% for Al, Mn, Mg, Na, P, and better than 6% for trace elements, with the exception of Ba (12%), Th (8%), and Nb (13%). Detection limits for trace elements are: Zn, Cu, Sc, Ga, Ba, Ce, Pb = 5 ppm; Ni, Co, Cr, V, Rb, Th, Nb, La, Sr, Zr, Y = 2 ppm. Accuracy for ICP-MS analyses ranges from 2 to 7 relative percent, with the exception of Nb (11%), Ta (14%), and U (12%). Detection limits (in ppm) are: Nb, Hf, Ta = 0.02; Th, U = 0.01; light (L-) and medium (M-) rare earth elements (REE) < 0.05; heavy REE (HREE) < 0.07.

Basalt geochemistry and tectono-magmatic interpretation

Ocean-floor hydrothermal processes commonly lead to a variable mobilization of large ion lithophile elements (LILE), such as Ba, Rb, K, and Sr. By contrast, the transition metals (e.g., V, Cr, Mn, Fe, Co, Ni, Zn) and high field strength elements (HFSE) (Zr, Y, Nb, Th, Ta, Ti, Hf, P) are relatively immobile, and largely reflect magmatic abundances (Beccaluva et al., 1979; Pearce and Norry, 1979; Shervais, 1982). REE are also relatively immobile during alteration processes, although LREE may be slightly mobile compared to HREE. For these reasons, the discussion on the geochemical and petrogenetic features of the studied rocks will be mainly based on those elements which can be considered immobile during metamorphic and alteration processes.

The studied basalts (SiO_2 = 52.02, 51.36) display a clear sub-alkaline nature, as exemplified by their Nb/Y ratios < 0.7 (Table E1). MgO (5.68, 7.25 wt%), CaO (8.75, 10.70wt%) contents, and Mg# (62.4, 63.4), indicate that these samples represent slightly evolved volcanic products. TiO_2 (1.34, 1.50wt%), P_2O_5 (0.12, 0.14wt%), Zr (77, 108 ppm), Y (26, 28 ppm) contents are relatively high. These basalts generally display low compatible element contents (Cr = 158, 180 ppm, Ni = 108, 158 ppm, Co = 50, 55 ppm). The distribution of HFSE concentrations (Fig. 7a) indicates that these rocks share affinities with ocean-floor basalts. In particular, elements from P to Yb exhibit flat patterns showing approximately 1 times N-MORB abundances (Sun and McDonough, 1989). Nonetheless, these basalts show a slight enrichment in Th, U, and Ta with respect to the typical N-MORB (Fig. 7a). REE patterns (Fig. 7b) are also consistent with N-MORB compositions. They have an overall enrichment in HREE of 13-20 times chondrite (Fig .7b). They are characterized by either mild LREE depletion or enrichment with respect to medium REE (La_N/Sm_N = 0.76, 1.07), but show a slight to moderate LREE/HREE enrichment (La_N/Yb_N = 1.09, 1.48). In accordance with their slightly evolved nature, no negative Eu anomaly can be observed (Fig. 7b).

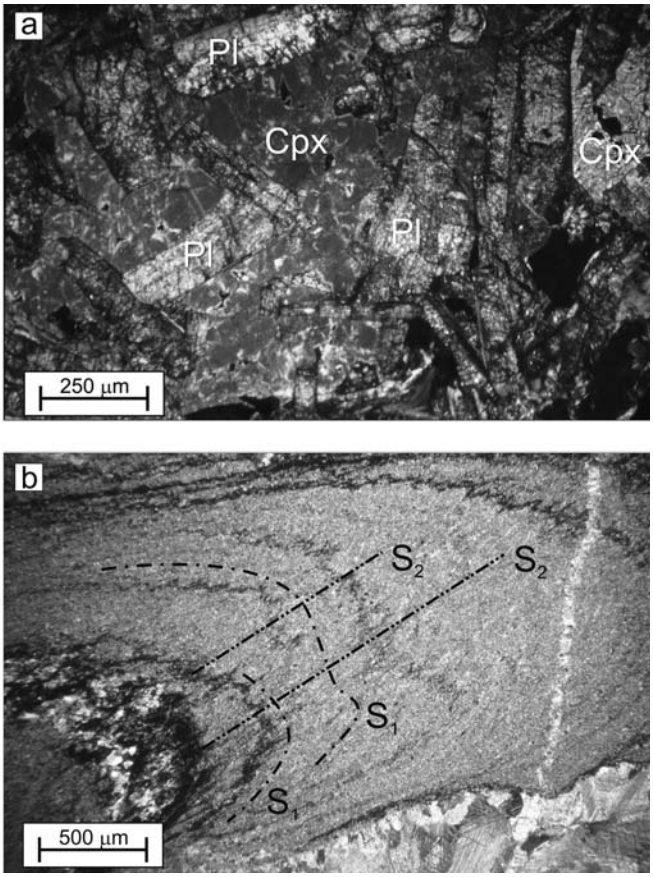

Fig. 6 - a- Photomicrograph (nicols +) of idiomorphic plagioclase and interstitial to poikilitic clinopyroxene in the dolerite of Figg. 4c, 5 (sample GRA11); b- Photomicrograph of metamorphic rock in the Sub-ophiolitic Mélange, photomicrograph (nicols +) of D_2 structure (sample GRA19).

Table 1 - Bulk rock major and trace element analyses of basalts from the Grammos-Arrenes area (samples GRA15-16).

Sample	GRA15		GRA16	
Rock Type	basalt N-MORB		basalt N-MORB	
	a	b	a	b
SiO_2	52.02		51.36	
TiO_2	1.50		1.34	
Al_2O_3	16.45		14.98	
Fe_2O_3	0.91		1.12	
FeO	6.10		7.46	
MnO	0.43		0.16	
MgO	5.68		7.25	
CaO	8.75		10.70	
Na_2O	3.95		3.79	
K_2O	1.84		0.19	
P_2O_5	0.14		0.12	
L.O.I.	1.97		1.58	
Total	99.75		100.04	
Mg#	62.4		63.4	
Zn	75		72	
Cu	99		88	
Sc	12		16	
Ga	18		21	
Ni	108		158	
Co	50		55	
Cr	180		158	
V	183		237	
Rb	38	36.5	4	1.99
Ba	564		174	
Nb	3	2.66	3	3.77
Hf		2.58		1.97
Ta		0.26		0.23
Th		0.29		0.23
U		0.08		0.09
Pb	7		6	
Sr	408	387	139	136
Zr	108		77	
Y	26	24.4	28	27.5
La	4	3.72	6	4.73
Ce	13	12.1	14	12.7
Pr		2.02		1.88
Nd		9.82		8.82
Sm		3.15		2.85
Eu		1.17		1.05
Gd		3.98		3.64
Tb		0.71		0.66
Dy		4.56		4.18
Ho		0.95		0.91
Er		2.64		2.42
Tm		0.40		0.36
Yb		2.45		2.29
Lu		0.36		0.32
Ti/V	50		35	
Nb/Y		0.10		0.13
$(La/Sm)_N$		0.76		1.07
$(Sm/Yb)_N$		1.43		1.38
$(La/Yb)_N$		1.09		1.48
Th/Ta		1.12		1.02
Th/Tb		0.41		0.36
Ce/Y		0.46		0.45
Nb/Yb		1.09		1.64

Samples location are reported in Figs.2, 3. N-MORB- normal-type mid-ocean ridge basalt; a- XRF analyses; b- ICP-MS analyses. Fe_2O_3- 0.15 x FeO; Mg#- 100 x Mg/(Mg+Fe^{2+}), where Mg- MgO/40 and Fe- FeO/72. Normalizing values for REE ratios are from Sun and McDonough (1989).

The Ti/V ratios are 35 and 50, which are typical values for basalts generated at mid-ocean ridge settings (Shervais, 1982). In the Zr/4-Y-2Nb (Meschede, 1986) and Th-Ta-Hf/3 (Wood, 1980) discrimination diagrams of Fig. 8, these basalts plot in the fields for N-MORB compositions.

Ratios of highly incompatible trace elements, such as Ce/Y are generally little influenced by moderate extents of fractional crystallization, and are believed to reflect either the source characteristics or the degree of partial melting (Saunders et al., 1988). Ce is more incompatible than Y; thus, rocks representing the smallest degree of partial melting or derived from more enriched sources exhibit both the highest Ce/Y ratios. The studied basalts exhibit very similar Ce/Y ratios (0.45, 0.46), which are, however, slightly higher than those of typical N-MORB (0.27) and slightly lower than those of typical E-MORB (0.68) (Sun and McDonough, 1989). Ce/Y ratios of the studied basalts are therefore compatible with a genesis either from primary magmas originating from slightly enriched N-MORB type sub-oceanic mantle sources or from low degree partial melting of a depleted N-MORB type mantle source. Hygromagmatophile elements are weakly fractionated by small extents of both partial melting and fractional crystallization. Therefore, hygromagmatophile element ratios (e.g., Th/Ta, Th/Tb) in basalts are believed to reflect the elemental ratios in their mantle sources. The studied basalts have very similar Th/Tb (0.36, 0.41) and Th/Ta (1.02, 1.12) ratios, which suggest that they most likely derived from compositionally very similar mantle sources. However, a comparison of these ratios and those observed in typical N-MORB (Th/Tb = 0.18 and Th/Ta = 0.91,

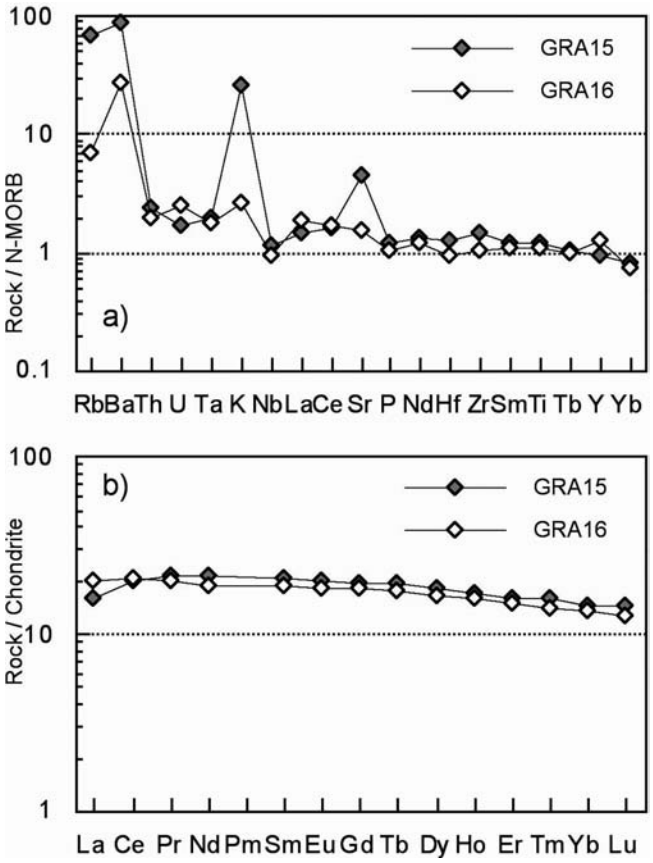

Fig. 7 - N-MORB normalized incompatible element (a) and chondrite-normalized REE (b) patterns for basalts from the Grammos-Arrenes area (samples GRA15-16). Normalizing values are from Sun and McDonough (1989).

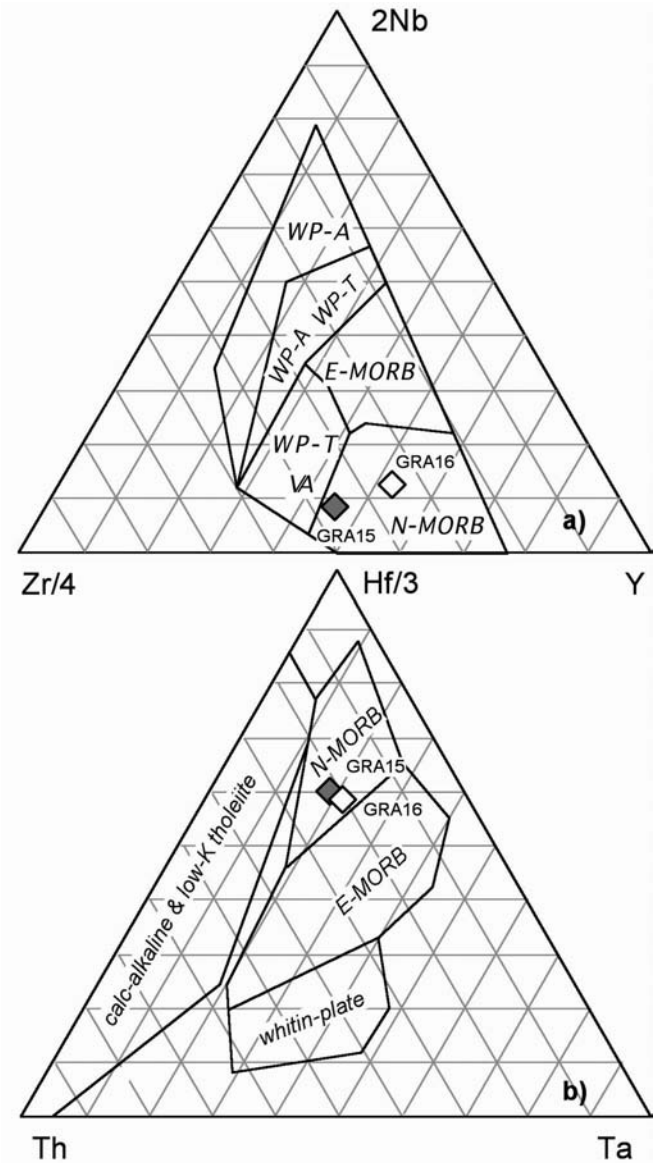

Fig. 8 - a- Zr/4-Y-2Nb (Meschede, 1986) and b) Th, Ta, Hf/3 (Wood, 1980) discrimination diagrams for basalts from the Grammos-Arrenes area (samples GRA15-16). Abbreviations: WP- within-plate; VA- volcanic arc; A- alkaline; T- tholeiite; N-MORB- normal-type mid-ocean ridge basalts; E-MORB- enriched-type mid-ocean ridge basalt.

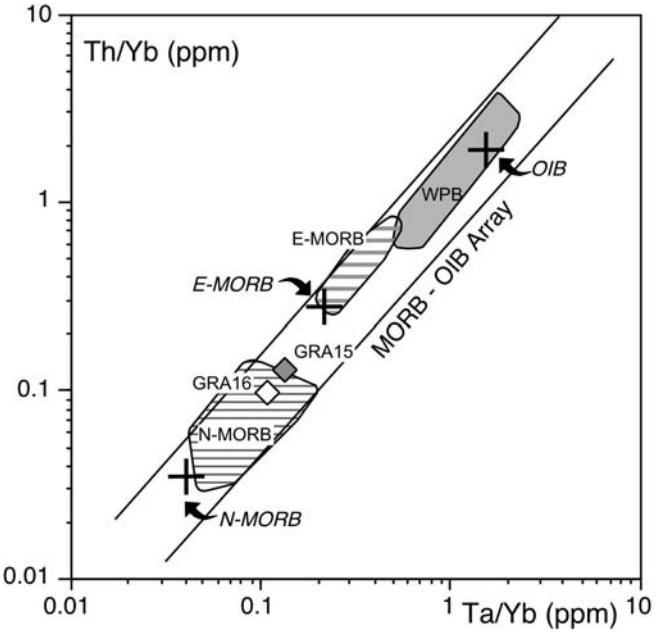

Fig. 9 - Th/Yb vs. Ta/Yb diagram for basalts from the Grammos-Arrenes area (samples GRA15-16). Compositions of Modern ocean-island basalt (OIB), enriched-type mid-ocean ridge basalt (E-MORB), and normal-type mid-ocean ridge basalt (N-MORB) are from Sun and McDonough (1989). Variations of elemental ratios of Triassic alkaline within-plate basalts (WPB), Triassic enriched-type mid-ocean ridge basalts (E-MORB) and Triassic-Jurassic normal-type mid-ocean ridge basalts (N-MORB) from various localities of the Hellenides are reported for comparison (data from Saccani and Photiades, 2005, and references therein).

Sun and McDonough, 1989) further supports the hypothesis that the Grammos-Arrenes basalts derived from a slightly enriched N-MORB type mantle source, as also indicated by the Th/Yb vs. Ta/Yb ratios plotted in Fig. 9. According to the model proposed by Haase and Devey (1996), their $(Dy/Yb)_N$ and $(Ce/Yb)_N$ compositions are compatible with low degree (4-5%) partial melting of a depleted MORB mantle source (Fig. 10). In summary, the chemistry of the Grammos-Arrenes basalts suggests a genesis in a mid-ocean ridge tectonic setting from low degree partial melting of a N-MORB type sub-oceanic mantle source.

RADIOLARIAN BIOSTRATIGRAPHY

We collected eight chert samples for radiolarian analyses: GRA3, 4, 8, 9, 10 associated withbasalt samples GRA6, 7 and GRA12, 13, 14 associated with basalt samples GRA15, 16 respectively (Fig. 5). All the samples were etched with hydrofluoric acid at different concentrations, using the method proposed by Dumitrica (1970) and Pessagno and Newport (1972). Probably due to the effects of strong recrystallization associated with shear zones, samples GRA3, 4, 8, 9 and 10 show very bad preservation that hampered an age determination. On the other hand, the samples collected in areas far from shear zones contain radiolarians with a good preservation (Plate 1); in particular sample GRA13 shows very well preserved radiolarians.

In this paper we utilize the zonation proposed by Baumgartner et al. (1995) that span the Middle Jurassic - Early Cretaceous time (Aalenian - early Aptian) and it includes 22 Unitary Association Zones (UAZ). These 22 UAZ represent a synthesis of the 127 unitary associations (UA) calculated utilizing the Biograph program (Savary and Guex, 1991).

Sample GRA12

Archaeodictyomitra sp. cf. *A. patricki* Kocher, *Archaeodictyomitra* sp. cf. *A. rigida* Pessagno, *Archaeodictyomitra* sp., *Archicapsa* sp., *Eucyrtidiellum* sp. cf. *E. circumperforatum* Chiari, Marcucci and Prela, *Eucyrtidiellum* sp. cf. *E. unumaense unumaense* (Yao), *Hexasaturnalis suboblongus* (Yao), *Hsuum* sp., *Praewilliriedellum robustum* (Matsuoka), *Saitoum levium* De Wever, *Saitoum* sp., *Stichocapsa japonica* Yao, *Striatojaponocapsa plicarum* (Yao), *Striatojaponocapsa* sp. cf. *S. plicarum* (Yao), *Svinitzium kamoensis* (Mizutani and Kido), *Williriedellum yaoi* (Kozur), *Williriedellum* sp. cf. *W. buekkense* (Kozur), *Williriedellum* sp. cf. *W. yaoi* (Kozur), *Unuma* sp.

AGE: latest Bajocian-early Bathonian (UAZ 5) for the occurrence of *Praewilliriedellum robustum* (Matsuoka) with *Striatojaponocapsa plicarum* (Yao) and *Hexasaturnalis*

suboblongus (Yao)

In this sample is present the taxon *Hexasaturnalis suboblongus* (Yao). After Dumitrica and Dumitrica-Jud (2005) the range of this taxon is early-middle Bajocian to late Bajocian (UAZ 3-4), whereas Chiari et al. (2007) indicated that the range could be longer: early-middle Bajocian to latest Bajocian-early Bathonian (UAZ 3-5).

Sample GRA13

Archaeodictyomitra rigida Pessagno, *Archaeodictyomitra* sp. cf. *A. rigida* Pessagno, *Eucyrtidiellum unumaense unumaense* (Yao), *Eucyrtidiellum* sp. cf. *E. unumaense unumaense* (Yao), *Eucyrtidiellum* sp., *Hexasaturnalis tetraspinus* (Yao), *Hsuum* sp., *Japonocapsa fusiformis* (Yao), *Japonocapsa* sp. cf. *J. fusiformis* (Yao), *Parahsuum* sp., *Praewilliriedellum* sp. cf. *P. robustum* (Matsuoka), *Saitoum levium* De Wever, *Saitoum* sp. cf. *S. levium* De Wever, *Saitoum* sp., *Stichocapsa japonica* Yao, *Striatojaponocapsa plicarum* (Yao), *Striatojaponocapsa* sp. cf. *S. plicarum* (Yao), *Svinitzium* sp. cf. *S. kamoensis* (Mizutani and Kido), *Transhsuum* sp. cf. *T. brevicostatum* (Ozvoldova), *Unuma echinatus* Ichikawa and Yao, *Unuma* sp., *Unuma* sp. cf. *U. echinatus* Ichikawa and Yao, *Williriedellum* sp. cf. *W. yaoi* (Kozur).

AGE: late Bajocian to latest Bajocian-early Bathonian (UAZ 4-5) for the occurrence of *Saitoum levium* De Wever, *Striatojaponocapsa plicarum* (Yao) with *Japonocapsa fusiformis* (Yao).

Sample GRA14

Archaeodictyomitra patricki Kocher, *Archaeodictyomitra rigida* Pessagno, *Archaeodictyomitra* sp., *Belleza decora* (Rüst), *Saitoum* sp., *Striatojaponocapsa plicarum* (Yao), *Svinitzium kamoensis* (Mizutani and Kido), *Svinitzium* sp. cf. *S. kamoensis* (Mizutani and Kido), *Transhsuum* sp., *Unuma* sp., *Unuma echinatus* Ichikawa and Yao, *Williriedellum* sp. cf. *W. yaoi* (Kozur), *Williriedellum* sp.

AGE: late Bajocian to latest Bajocian-early Bathonian (UAZ 4-5) for the occurrence of *Striatojaponocapsa plicarum* (Yao) and *Belleza decora* (Rüst).

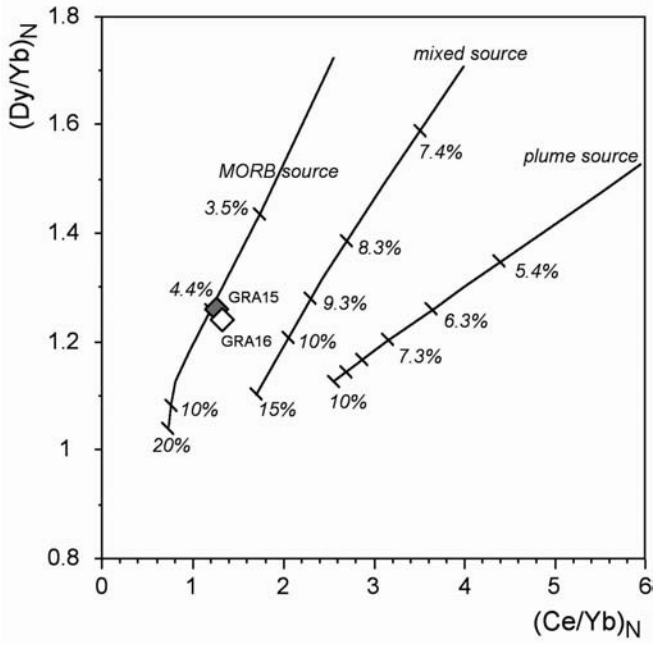

Fig. 10 - $(Dy/Yb)_N$ vs. $(Ce/Yb)_N$ diagram for basalts from the Grammos-Arrenes area (samples GRA15-16). Melt model is from Haase and Dewey (1996).

FINAL REMARKS

The radiolarian cherts associated with N-MORB basalts sampled in the Sub-ophiolitic Mélange of the Grammos-Arrenes area are latest Bajocian-early Bathonian in age (UAZ 5). This datum is consistent with others from the Sub-ophiolitic Mélange: Argolis (Bortolotti et al., 2003; Baumgartner 1984; 1985; 1995), Othris (Bortolotti et al., 2008), Eubea (Danelian and Robertson, 2001), as well as from the Ophiolitic Nappe: Vourinos (Chiari et al., 2003), Eubea (Schereikes et al., 2010).

The dolerite in the Sub-ophiolitic Mélange (Fig. 5) at times clearly intrudes whereas in other cases encloses a limestone sequence, while its contact with the volcano-sedimentary cover of the ophiolites is unclear, possibly tectonic. Different hypotheses can be proposed to explain this situation: a- the dolerite intruded the mélange sequence, where the limestones were associated with radiolarian cherts and basalts; b- the dolerite intruded a limestone sequence, probably pertaining to a continental margin, and was then incorporated in the Sub-ophiolitic Mélange as a block and associated with the ophiolitic volcano-sedimentary cover. Although very rare, both situations have been documented in the Dinaric-Hellenic Chain. Saccani and Photiades (2005) documented the occurrence of both boninitic and MORB dykes cutting the sedimentary structures of the sub-ophiolitic mélange (Rubik Complex) in northern Albania. These dykes were interpreted as injections of magmas in the fore-arc region where the tectono-sedimentary mélange was forming. By contrast, Ghikas et al. (2010) described the occurrence of dolerite and gabbro dykes intruding Triassic continental margin carbonate sequences. These intrusions have been interpreted as the earliest magmatic events that accompanied the continental rift and break up. The data here presented do not allow a clear definition of the tectonic significance of the dolerite intrusion in the Grammos-Arrenes area and further investigations will be necessary.

The basalts studied in this paper record a step of the Middle Jurassic oceanic evolution in the Hellenides. In fact, their N-MORB geochemistry implies that a mid-ocean ridge was still active in this sector of the Neo-Tethys during this time. However, most of the N-MORBs from the external ophiolite belt are Triassic in age (Bortolotti et al., 2004a; 2008), while Middle Jurassic N-MORBs (Chiari et al., 2002) are volumetrically subordinate. Moreover, though the age of N-MORBs from the external ophiolite belt is not well constrained, the occurrence of both Triassic and Middle Jurassic N-MORBs has also been reported in this ophiolite belt (see Pe-Piper and Piper, 2002; Saccani et al., 2008a for references).

While it is commonly accepted that the Triassic N-MORBs record the main mid-ocean ridge spreading phase of the Neo-Tethys, the geodynamic significance of Middle Jurassic N-MORBs is still matter of debate. In fact, according to many authors (e.g., Robertson, 2002; Bortolotti and Principi, 2005; Dilek et al., 2008; Saccani et al., 2010), the Neo-Tethys was largely dominated by convergent movements with the development of intra-oceanic island arcs in supra-subduction zone settings (SSZ) since the Early-Middle Jurassic, as deduced from the massive occurrence of SSZ-type ophiolites in both the external (Saccani et al.,

2010) and internal (Saccani et al., 2008a; 2008b; 2010) ophiolite belts.

All along the westernmost side of the external ophiolite belt, from northern Albania (Bortolotti et al., 1996; 2002; Bébien et al., 2000) to southern Albania (Hoeck et al., 2002), Pindos (Saccani and Photiades, 2004), and Othrys (Photiades et al., 2003; Saccani and Photiades, 2005; Barth et al., 2008; Barth and Gluhak, 2009), most of the Middle Jurassic N-MORBs are closely associated in space and time with SSZ-type ophiolites, such as boninitic volcanics and medium-Ti basalts (MTB). In particular, in the neighbouring areas (i.e., southern Albania and Aspropotamos Complex in the Pindos Massif) the Middle-Jurassic N-MORBs are stratigraphically associated with boninite volcanics and MTBs (Hoeck et al., 2002; Saccani and Photiades, 2004). For explaining this close association of N-MORBs and SSZ-type volcanics in the external ophiolites many authors have suggested, thought with some variants, that most of the N-MORBs of this belt formed in a SSZ setting (Bortolotti et al., 1996; 2002; Bébien et al., 2000; Robertson and Shallo, 2000; Barth et al., 2008; Barth and Gluhak, 2009). A comparison with similar rocks from the Aspropotamos series of the Pindos ophiolites (Saccani and Photiades, 2004) indicatesthat the N-MORBs from the Grammos-Arrenes area record the Middle Jurassic evolution of a mid-ocean spreading ridge located near to or within a SSZ setting.

The present tectonic stack represents the result of a long-lasting tectonic history. The tectonic slices of Beotian Flysch below the Sub-ophiolitic Mélange testify an eastern provenance of the Ophiolitc Nappe that during its westward emplacement onto the continental margin scraped off portions of sequences that are now juxtaposed to more external units (i.e., Pindos Flysch). The westward movement of the oceanic units onto the Pindos Flysch ended only during the latest Eocene-Early Oligocene, when a climax of compressional deformation lead to the formation of eastward verging reverse faults, followed by strike slip movements (Zelilidis et al., 2002, Vamvaka et al., 2006), that cut the Ophiolitic Nappe + Sub-ophiolitic Mélange basal thrust and led to inversion tectonics in the western border of the Meso-Hellenic Basin (Ferrière et al., 2004).

ACKNOWLEDGMENTS

This study was supported by funds from the Italian Ministry of University, University of Florence, University of Ferrara, CNR - Istituto di Geoscienze e Georisorse. Renzo Tassinari his gratefully acknowledged for assistance with XRF and ICP-MS analyses. Radiolarian micrographs were taken with a Zeiss EVO MA15 of the MEMA by Maurizio Ulivi, University of Florence.

Many thanks go to Paulian Dumitrica and Michele Marroni for their helpful revisions.

REFERENCES

Ananiadis G., Vakalas I., Zelilidis A. and Stoykova K., 2004. Palaeographic evolution of Pindos Basin during Paleogene using calcareous nannofossils. Bull. Geol. Soc. Greece, 36, 836-845.

Aubouin J., 1959. Contribution à l'étude géologique de la Grèce septentrionale: les confins de l'Epire et de la Thessalie. Ann. Géol. Pays Hellén., 10: 1-483.

Barth M.G., Mason P.R.D., Davies G.R. and Drury M.R., 2008. The Othris ophiolite (Greece): A snapshot of subduction initiation at a mid-ocean ridge. Lithos, 100: 234-254.

Barth M.G. and Gluhak T.M., 2009. Geochemistry and tectonic setting of mafic rocks from the Othris Ophiolite, Greece. Contrib. Mineral. Petrol., 157: 23-40.

Baumgartner P.O., 1984. A Middle Jurassic-Early Cretaceous low-latitude radiolarian zonation based on Unitary Associations and age of Tethyan radiolarites. Ecl. Geol. Helv., 77: 729-837.

Baumgartner P.O., 1985. Jurassic sedimentary evolution and nappe emplacement in the Argolis Peninsula (Peloponnesus, Greece). Mém. Soc. Helv. Sci. Nat., 99: 1-111.

Baumgartner P.O., 1995. Towards a Mesozoic radiolarian database - Updates of the work 1984-1990. In: P.O. Baumgartner et al. (Eds.), Middle Cretaceous to Lower Cretaceous radiolaria of Tethys: occurrences, systematics, biochronology. Mém. Géol., Lausanne, 23: 689-700.

Baumgartner P.O., Bartolini A. Carter E.S., Conti M., Cortese G., Danelian T., De Wever P., Dumitrica P., Dumitrica-Jud R., Goričan Š., Guex J., Hull D.M., Kito N., Marcucci M., Matsuoka A., Murchey B., O'Dogherty L., Savary J., Vishnevskaya V., Widz D. and Yao A., 1995b. Middle Jurassic to Early Cretaceous Radiolarian biochronology of Tethys based on Unitary Associations. In: P.O. Baumgartner et al. (Eds.), Middle Jurassic to Lower Cretaceous Radiolaria of Tethys: occurrences, systematics, biochronology, Mém. Géol., Lausanne, 23: 1013-1048.

Bébien J., Dimo-Lahitte A., Vergély P., Insergueix-Filippi D. and Dupeyrat L., 2000. Albanian ophiolites. I - Magmatic and metamorphic processes associated with the initiation of a subduction. Ofioliti, 25: 39-45.

Beccaluva L., Ohnenstetter D. and Ohnenstetter M., 1979. Geochemical discrimination between ocean-floor and island-arc tholeiites-application to some ophiolites. Can. J. Earth Sci., 16: 1874-1882.

Bernoulli D. and Laubscher H. 1972. The palinspastic problem of the Hellenides. Ecl. Geol. Helv., 65: 107-118.

Blanchet R., Cadet J.P., Charvet J. and Rampnoux J.P., 1969. Sur l'existence d'un important domaine du flysch tithonique - crétacé inférieur en Yougoslavie: l'unité du Flysch Bosniaque. Bull. Soc. Géol. France, 11 (7): 871-880.

Bortolotti V., Carras N., Chiari M., Fazzuoli M., Marcucci M., Nirta G., Principi G. and Saccani E., 2009. The ophiolite-bearing mélange in the Early Tertiary Pindos Flysch of Etolia (Central Greece). Ofioliti, 34 (2): 83-94.

Bortolotti V., Carras N., Chiari M., Fazzuoli M., Marcucci M., Photiades A. and Principi G., 2003. The Argolis Peninsula in the palaeogeographic and geodynamic frame of the Hellenides. Ofioliti, 28: 79-94.

Bortolotti V., Chiari M., Kodra A., Marcucci M., Mustafa F., Principi G. and Saccani E., 2004a. New evidence for Triassic MORB magmatism in the northern Mirdita Zone ophiolites (Albania). Ofioliti, 29: 243-246.

Bortolotti V., Chiari M., Marcucci M., Marroni M., Pandolfi L., Principi G. and Saccani E., 2004. Comparison among the Albanian and Greek ophiolites, in search of constraints for the evolution of the Mesozoic Tethys Ocean. Ofioliti, 29:19-35

Bortolotti V., Chiari M., Marcucci M., Photiades P., Principi G. and Saccani E., 2008. New geochemical and age data on the ophiolites from the Othrys area (Greece): implication for the Triassic evolution of the Vardar Ocean. Ofioliti, 33: 135-151.

Bortolotti V., Kodra A., Marroni M., Mustafa F., Pandolfi L., Principi G. and Saccani E., 1996. Geology and petrology of ophiolitic sequences in the Mirdita region (Northern Albania). Ofioliti, 21: 3-20.

Bortolotti V., Marroni M., Pandolfi L., Principi G. and Saccani E., 2002. Interaction between mid-ocean ridge and subduction magmatism in Albanian ophiolites. J. Geol., 110: 561-576.

Bortolotti V.and Principi G., 2005. Tethyan ophiolites and Pangea break-up. Island Arc, 14: 442-470.

Brunn H.J., 1956. Contribution à l'étude géologique du Pinde septentrional et d'une partie de la Macedonie occidentale. Ann.

Géol. Pays Hellén., 7: 1-358.
Chiari M., Bortolotti V., Marcucci M., Photiades A. and Principi G., 2003. The Middle Jurassic siliceous sedimentary cover at the top of the Vourinos ophiolite (Greece). Ofioliti, 28: 95-103.
Chiari M., Cobianchi M. and Picotti V., 2007. Integrated stratigraphy (radiolarians and calcareous nannofossils) of the Middle to Upper Jurassic Alpine radiolarites (Lombardian Basin, Italy): Constraints to their genetic interpretation. Palaeo. Palaeo. Palaeo., 249: 233-270.
Chiari M., Marcucci M. and Prela M., 2002. New species of Jurassic radiolarian in the sedimentary cover of ophiolites in the Mirdita area, Albania. Micropal., 48: 61-87.
Danelian T. and Robertson A.H.F., 1998. Palaeogeographic implications of the age of radiolarian rich sediments in Beotia (Greece). Bull. Geol. Soc. Greece, 32 (2): 21-29.
Danelian T. and Robertson A.H.F., 2001. Neotethyan evolution of eastern Greece (Pagondas Mélange, Evia Island) inferred from radiolarian biostratigraphy and the geochemistry of associated extrusive rocks. Geol. Mag., 138: 345-63
De Bono A., 1998. Pelagonian margins in Central Evia Island (Greece). Stratigraphy and geodynamic evolution, Univ. Lausanne, Unpubl. Ph-D Thesis.
Dilek Y., Shallo M. and Furnes H., 2008. Geochemistry of the Jurassic Mirdita Ophiolite (Albania) and the MORB to SSZ evolution of a marginal basin oceanic crust. Lithos, 100: 174-209.
Dumitrica P., 1970. Cryptocephalic and cryptothoracic Nassellaria in some Mesozoic deposits of Romania. Rev. Roum. Géol., Géophys., Géograph. (Sér. Géol.), 14: 45-124.
Dumitrica P. and Dumitrica-Jud R., 2005. *Hexasaturnalis nakasekoi* nov. sp., a Jurassic saturnalid radiolarian species frequently confounded with *Hexasaturnalis suboblongus* (Yao). Rev. Micropal., 48: 159-168.
Ferrière J., Reynaud J.-Y., Pavlopoulos A., Bonneau M., Migiros G., Chanier F., Proust J.-N. and Gardin S., 2004. Geologic evolution and geodynamic controls of the Tertiary intramontane piggyback Meso-Hellenic Basin, Greece. Bull. Soc. Géol. France, 175: 361-381.
Gardin S., Kici V., Marroni M., Pandolfi L., Pirdeni A. and Xhomo A., 1996. Litho- and biostratigraphy of the Firza Flysch, ophiolite Mirdita Nappe, Albania. Ofioliti, 21: 47-54.
Ghikas G., Dilek Y. and Rassios A.E., 2010. Structure and tectonics of subophiolitic mélanges in the western Hellenides (Greece): implications for ophiolite emplacement tectonics. Intern. Geol. Rev., 52: 423-453.
Hoeck V., Koller F., Meisel T., Onuzi K. and Kneringer E., 2002. The Jurassic South Albanian ophiolites: MOR- vs. SSZ-type ophiolites. Lithos, 65: 143-164.
IGME - Institute of Geology and Mineral Exploration of Greece, 1985. Geological Map of Greece, 1:50000: Chionades-Grammos Sheet.
IGME - Institute of Geology and Mineral Exploration of Greece, 1987. Geological Map of Greece, 1:50000: Konitsa Sheet.
Haase K.M. and Devey C.W., 1996. Geochemistry of lavas from the Ahu and Tupa volcanic fields, Easter hotspot, southeast Pacific: implications for intraplate magma genesis near a spreading axis. Earth Planet. Sci. Lett., 137: 129-143.
Jones G. and Robertson A.H.F., 1990. Tectono-stratigraphy and palaeogeographic evolution of the Mesozoic Pindos ophiolite and related units, northwestern Greece: an integrated supra-subduction zone spreading and subduction-accretion model., J. Geol. Soc. London, 148: 267-288.
Lachance G.R. and Trail R.J., 1966. Practical solution to the matrix problem in X-ray analysis. Can. Spectr., 11: 43-48.
Marroni M., Pandolfi L., Onuzi K., Palandri S. and Xhomo A., 2009. Ophiolite-bearing Vermoshi Flysch (Albanian Alps, Northern Albania): elements for its correlation in the frame of Dinaric-Hellenic Belt. Ofioliti, 34 (2): 95-108.
Meschede M., 1986. A method of discriminating between different types of mid-Ocean ridge basalts and continental tholeiites with the Nb-Zr-Y diagram. Chem. Geol., 56: 207-218.
Moores E., 1969. Petrology and structure of the Vourinos ophiolite complex of Northern Greece. Geol. Soc. Am. Spec. Paper, 118: 1-74.
Pearce J.A., 1982. Trace element characteristics of lavas from destructive plate boundaries. In: R.S. Thorpe (Ed.), Andesites. Wiley and Sons, New York, p. 525-548.
Pearce J.A. and Norry M.J., 1979. Petrogenetic implications of Ti, Zr, Y, and Nb variations in volcanic rocks. Contrib. Mineral. Petrol., 69: 33-47.
Pe-Piper G. and Piper D.J.W., 2002. The igneous rocks of Greece. The anatomy of an orogen. Gebrueder Borntraeger, Berlin, 573 pp.
Pessagno E.A. and Newport R.L., 1972. A technique for extracting Radiolaria from radiolarian cherts. Micropal., 18 (2): 231-234.
Photiades A., Saccani E. and Tassinari R., 2003. Petrogenesis and tectonic setting of volcanic rocks from the Subpelagonian ophiolitic mélange in the Agoriani area (Othrys, Greece). Ofioliti, 28: 121-135.
Richter D. and Müller C., 1992. Die Flysch-Zonen Griechenlands, VIII Neue Vorkommen von Böotischem Flysch im nördlichen Pindos-Gebirge (Griechenland), Z. Dt. Geol. Ges. Band, 143: 87-94.
Robertson A.H.F. and Shallo M., 2000. Mesozoic - Tertiary tectonic evolution of Albania in its regional Eastern Mediterranean context. Tectonophysics, 316: 197-214.
Robertson A.H.F., 2002. Overview of the genesis and emplacement of Mesozoic ophiolites in the Eastern Mediterranean Tethyan region. Lithos, 65: 1-67.
Robertson A.H.F., Clift P.D., Degnan P.J. and Jones G., 1991. Paleogeographic and paleotectonic evolution of the Eastern Mediterranean Neotethys. In: L.F. Jansa (Ed.), Paleogeography and paleoceanography of Tethys. Palaeo. Palaeo. Palaeo., 87: 289-343.
Saccani E. and Photiades A., 2004. Mid-ocean ridge and supra-subduction affinities in the Pindos Massif ophiolites (Greece): Implications for magma genesis in a proto-forearc setting. Lithos, 73: 229-253.
Saccani E. and Photiades A., 2005. Petrogenesis and tectono-magmatic significance of volcanic and subvolcanic rocks in the Albanide-Hellenide ophiolitic mélanges. Island Arc, 14: 494-516.
Saccani E., Beccaluva L., Photiades A. and Zeda O., 2010. Petrogenesis and tectono-magmatic significance of basalts and mantle peridotites from the Albanian-Greek ophiolites and subophiolitic mélanges. New constraints for the Triassic-Jurassic evolution of the Neo-Tethys in the Dinaride sector. Lithos, doi:10.1016/j.lithos.2010.10.009.
Saccani E., Photiades A., Santato A. and Zeda O., 2008a. New evidence for supra-subduction zone ophiolites in the Vardar Zone of northern Greece: implications for the tectono-magmatic evolution of the Vardar oceanic basin 2008. Ofioliti, 33 (1): 65-85.
Saccani E., Bortolotti V., Marroni M., Pandolfi L., Photiades A. and Principi G., 2008b. The Jurassic association of backarc basin ophiolites and calc-alkaline volcanics in the Guevgueli Complex (Northern Greece): implication for the evolution of the Vardar Zone. Ofioliti, 33 (2): 209-227.
Saunders A.D., Norry M.J. and Tarney J., 1988. Origin of MORB and chemically-depleted mantle reservoirs: Trace element constraints. In: M.A. Menzies and K.G. Cox (Eds.), Oceanic and continental lithosphere: Similarities and differences. J. Petrol., Spec. Vol., p. 414-445.
Savary J. and Guex J., 1991. BioGraph: un noveau programme de construction des corrélations biochronologiques basées sur les associations unitaires. Bull. Soc. Vaudoise Sci. Nat., 80 (3): 317-340.
Searle M.P. and Cox J., 1999. Tectonic setting, origin and obduction of the Oman ophiolite. Bull. Geol. Soc. Am., 111: 104-122.
Scherreikes R., Bosence D., Boudagher M., Melendez G. and Baumgartner P.O., 2010. Evolution of the Pelagonian carbonate platform complex and the adjacent oceanic realm in response to plate tectonic forcing (Late Triassic and Jurassic), Evvoia, Greece. Intern. J. Earth. Sci., 99 (6): 1317-1334.

Shervais J.W., 1982. Ti-V plots and the petrogenesis of modern ophiolitic lavas. Earth Planet. Sci. Lett., 59: 101-118.

Smith A.G., Hynes A.J., Menzies M., Nisbet E.G., Price I., Welland M.J. and Ferrière J., 1975. The stratigraphy of the Othris Mountains, Eastern Central Greece: a deformed Mesozoic continental cargin sequence. Ecl. Geol. Helv., 68: 463-481.

Spray J.G., Bebien J., Rex D.C. and Roddick J.C., 1984. Age constraints on the igneous and metamorphic evolution of the Hellenic-Dinaric ophiolites. In: J.E. Dixon and A.H.F. Robertson (Eds.), The geological evolution of the Eastern Mediterranean. Geol. Soc. London Spec. Publ., 17: 616-627.

Sun S.-S. and McDonough W.F., 1989. Chemical and isotopic-systematics of oceanic basalts: implications for mantle composition and processes. In: A.D. Saunders and M.J. Norry (Eds.), Magmatism in the ocean basins. Geol. Soc. London Spec. Publ., 42: 313-345.

Terry J. and Mercier M., 1971. Sur l'existence d'une série détritique berriasienne intercalée entre la nappe des ophiolites et le flysch éocène de la nappe du Pinde (Pinde septentrional, Grèce). C.R. S. Soc. Géol. France, 2: 71 -73.

Thiébault F., Fleury J.J., Clement B. and Degardin J.M., 1994. Paleogeographic and paleotectonic implications of clay mineral distribution in Late Jurassic-Early Cretaceous sediments of the Pindos-Olonos and Beotian Basins, Greece. Palaeo. Palaeo. Palaeo., 108: 23-40.

Vamvaka A., Kilias A., Mountrakis D. and Papaoikonomou J., 2006. Geometry and structural evolution of the Mesohellenic Trough (Greece): a new approach. Geol. Soc. London Spec. Publ., 260: 521-538.

Wood D.A., 1980. The application of a Th-Hf-Ta diagram to problems of tectonomagmatic classification and to establishing the nature of crustal contamination of basaltic lavas of the British Tertiary volcanic province. Earth Planet. Sci. Lett., 50: 11-30.

Zelilidis A., Piper D. J. W. and Kontopoulos N., 2002. Sedimentation and basin evolution of the Oligocene-miocene mesohellenic basin, Greece. A.A.P.G. Bull., 86 (1): 161-182.

Received, July 20, 2010
Acceptd, December 10, 2010

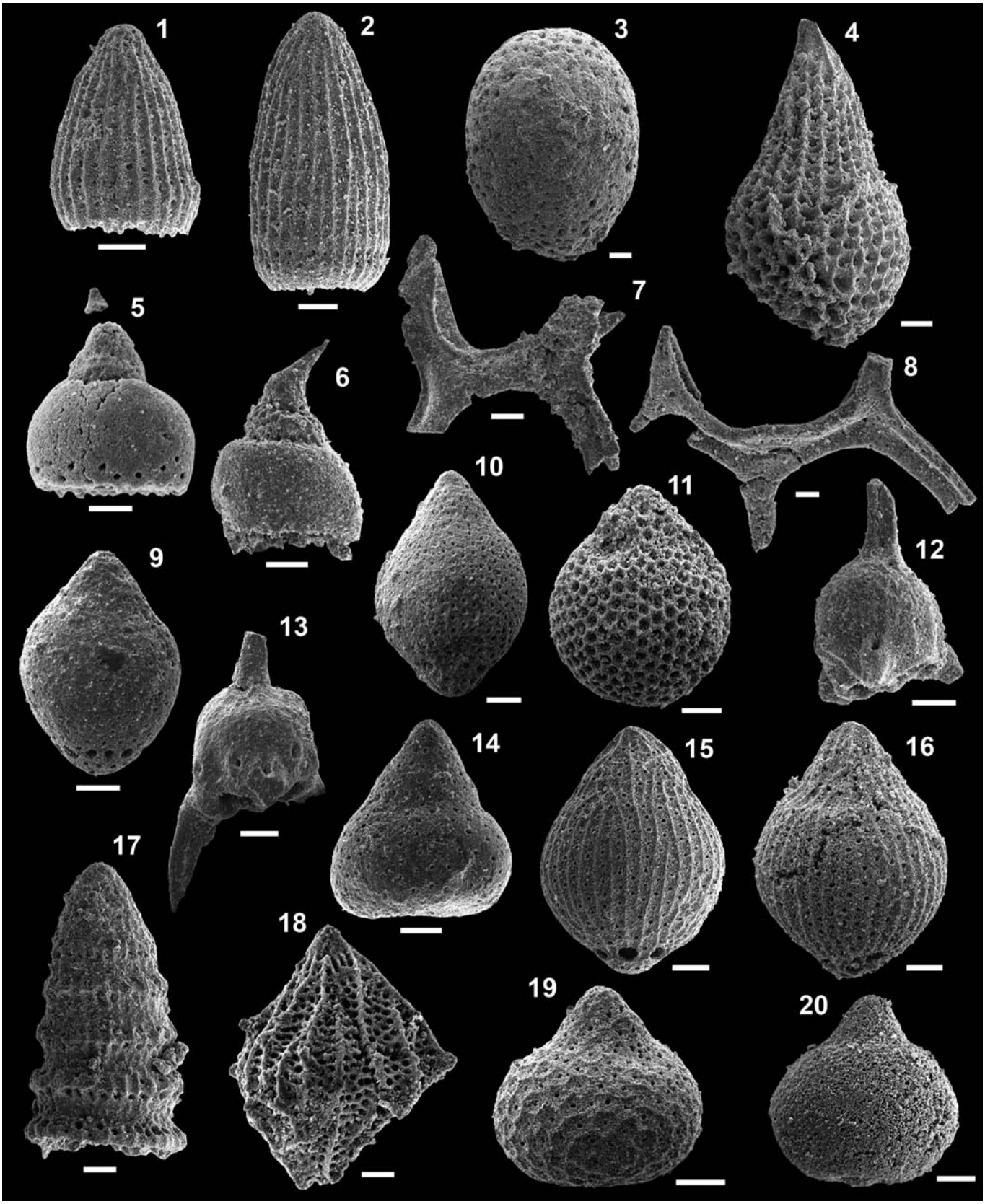

Plate 1 - 1) Archaeodictyomitra patricki Kocher, GRA14; 2) Archaeodictyomitra rigida Pessagno, GRA14; 3) Archicapsa sp., GRA12; 4) Belleza decora (Rüst), GRA14; 5) Eucyrtidiellum unumaense unumaense (Yao), GRA13; 6) Eucyrtidiellum sp. cf. E. unumaense unumaense (Yao), GRA12; 7) Hexasaturnalis suboblongus (Yao), GRA12; 8) Hexasaturnalis tetraspinus (Yao), GRA13; 9) Japonocapsa fusiformis (Yao), GRA13; 10) Japonocapsa fusiformis (Yao), GRA13; 11) Praewilliriedellum robustum (Matsuoka), GRA12; 12) Saitoum levium De Wever, GRA12; 13) Saitoum levium De Wever, GRA13; 14) Stichocapsa japonica Yao, GRA13; 15) Striatojaponocapsa plicarum (Yao), GRA14; 16) Striatojaponocapsa plicarum (Yao), GRA12; 17) Svinitzium kamoensis (Mizutani and Kido), GRA14; 18) Unuma echinatus Ichikawa and Yao, GRA13; 19) Williriedellum yaoi (Kozur), GRA12; 20) Williriedellum sp., GRA14. Scale bar = 20μ.